A comparative mineralogical and geochemical study of sulfide mine tailings at two sites in New Mexico, USA

Michelle P. Boulet · Adrienne C. L. Larocque

Abstract A comparative study of sulfide mine tailings from two sites near Silver City in southwest New Mexico has shown the need for environmental monitoring in a geological context. The Cyprus-Piños Altos and Cleveland deposits consist of Cu and Zn skarn mineralization in the Piños Altos Mountains of New Mexico. Primary ore minerals in both deposits include chalcopyrite, sphalerite, and galena. The Cyprus-Piños Altos Mine ceased operation in 1995 and the Cleveland Mill closed in 1950. The deposits have similar mineralogical characteristics; however, the tailings are different in terms of age, degree of oxidation and method of disposal. The Cyprus-Piños Altos tailings (CPAT) are stored in a lined, bermed impoundment. They are dominantly water-saturated and exhibit no secondary-phase formation. The grains are not cemented and show no evidence of primary-mineral dissolution. The geochemical data show a predominantly primary signature. The tailings pond water is neutral to slightly alkaline (pH from 7 to 8.3), partly as a result of processing methods. The Cleveland mill tailings (CMT) were deposited in a valley at the headwaters of an ephemeral stream. They are highly oxidized and differentially cemented. They have undergone numerous wet/dry cycles resulting in extensive oxidation. Secondary minerals predominate, and consist mainly of jarosite, goethite, hematite, and Fe-oxyhydroxides and -oxyhydroxysulfates. The pH of the stream draining the CMT is as high as 2.15. Maximum metal contents in the stream immediately downstream from the tailings are 5305 ppm Zn, 454 ppm Cu, 1.16 ppm Pb, 17.5 ppm Cd, 1.4 ppm As, and 0.01 ppm Hg.

Key words Cleveland mine · Cyprus-Piños Altos mine · Deming mill · Mill-tailings · Sulfide oxidation · Acid mine drainage

Received: 31 October 1996 · Accepted: 21 May 1997

M. P. Boulet · A. C. L. Larocque (✉)
Department of Geological Sciences, University of Manitoba, Winnipeg, Manitoba, R3T 2N2 Canada

Introduction

A comparative mineralogical and geochemical study of sulfide mine tailings from the Cyprus-Piños Altos mine tailings (CPAT) and Cleveland mill tailings (CMT) in southwest New Mexico (Fig. 1) has shown that a geological perspective on this environmental problem is necessary. Geochemical studies have shown mine tailings to be of environmental concern, as well as a future source for additional revenue through reprocessing. Mine-tailings mineralogy is complex and multiphase, and is a function of the type of deposit, grade of ore, proportion of sulfides, and buffering capacity of the tailings, as well as local and regional climate (temperature and precipitation). According to the classification of Jambor and Owens (1993, unpub. report), tailings mineralogy is divided into four categories: primary, secondary, tertiary, and quaternary. Primary minerals are those that have been finely crushed, mill-processed and deposited in the tailings pile, but remain unaltered. Secondary minerals are formed

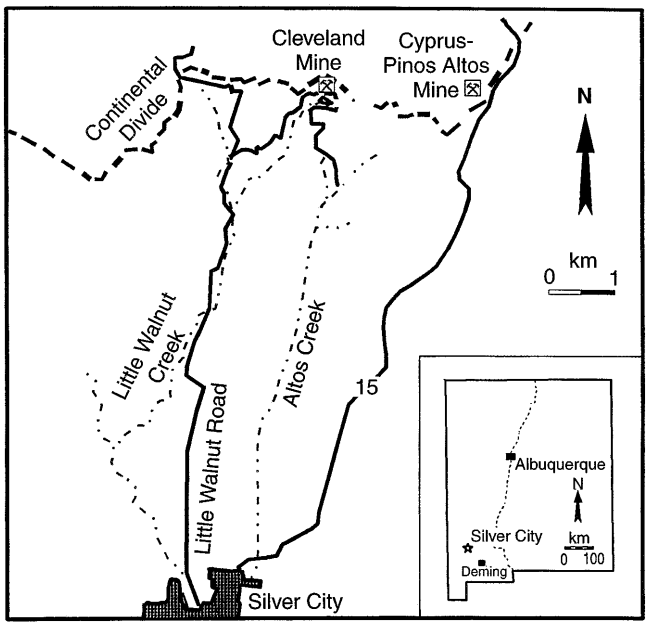

Fig. 1
Location map of Cleveland mine and mill site, Cyprus-Piños Altos mine and Deming mill; inset is a map of New Mexico, USA

within the impoundment by chemical weathering reactions. Tertiary minerals form during the drying of tailings samples once they have been removed from the impoundment, typically by precipitation from pore water. Quaternary minerals form as result of surface oxidation of the tailings samples during storage, after the samples have dried.

Mineralogical studies of mine tailings are important for environmental applications because most ore minerals are very sensitive to changes in environmental conditions, especially temperature, humidity, pH, and Eh. Elements released by oxidation and dissolution of primary ore minerals may be incorporated into secondary minerals by precipitation, sorption or ion exchange, or they may be removed from the tailings in solution, thereby contaminating surface and groundwater. With a thorough understanding of the chemical reactions and mineral transformations that occur in tailings, along with knowledge of the mineralogy and mineral chemistry of the primary assemblage, it is possible to predict the toxicity of the mine tailings. This is the first step in preventing mobilization of metals in our environment and in effectively remediating existing sites.

Over half a million tonnes of tailings from the Cyprus-Piños Altos mine have been deposited at the Deming mill since 1990. The tailings were deposited in a polyethylene-lined bermed impoundment beginning in 1992; prior to 1992 the tailings were deposited in an unlined pond. The principle elements processed were Cu, Fe, Pb and Zn, with Au and Ag by-products. Table 1 shows the average head grades and tailings grades. The CMT were deposited in a valley at the headwaters of an ephemeral stream at the mill site. The Cleveland mine site was actively mined from 1915 to 1945 and periodically mined from 1945 to 1950, at which time the mine closed (Soulé 1948; Anderson 1957); the site has since been abandoned. The mine was located approximately 500 m northeast of the mill site. The main tailings pile has a total volume of 22900 m^3 (U.S. EPA 1993, unpub. report) and is subdivided into the east pile and west pile. At the Cleveland mine, the principle elements mined were Zn, Cu, Pb, and Fe with Au and Ag by-products. Table 2 shows the range of head grades from 1915 to 1945, and the average tailings grades as of 1995. The U.S. Environmental Protection Agency (U.S. EPA) has declared the Cleveland mill tailings a Superfund site due to the occurrence of high concentrations of As in the tailings.

Table 1
Head and tailings grades for the Cyprus-Piños Altos mine in 1995 (Ore values from Albert Arrey, formerly of Cyprus Piños Altos Corporation, pers. comm. 1995)

Element	Ore grade	Tailings grade
Cu	5%	0.15%
Fe	15%	11%
Pb	0.074%	0.6%
Zn	0.21%	0.065%
Ag	44.3 g/tonne	10.2 g/tonne
Au	0.62 g/tonne	0.093 g/tonne

Table 2
Range of head grades from 1915–1945 and average tailings grades from 1995 for the Cleveland mine (Ore values from Soulé (1948), tailing samples collected in 1995)

Element	Ore grade	Tailings grade
Cu	0.2–0.563%	0.061%
Fe	not available	17.21%
Pb	0.517–2.2%	0.0058%
Zn	8.9–14.9%	0.12%
Ag	46–131 g/tonne	53.7 g/tonne
Au	0.062–0.31 g/tonne	0.056 g/tonne

The Piños Altos mine and mill ceased operation in 1995. The Cleveland mine and mill closed in 1950. The deposits have similar gross mineralogical characteristics; however, the tailings are different in terms of age, degree of oxidation and style of disposal. The focus of this paper is to identify residence sites of transition metals at the mineralogical scale and mine tailings scale, and relate mineral transformations that occur during weathering to the generation and composition of acidic drainage.

Geographic and geological setting

The Piños Altos mining district, Grant County, New Mexico, contains many mines, most of which were active in the mid to late 1800s and early 1900s. This historic mining district is centered on the Piños Altos Mountains, approximately 13 km north of Silver City. Both the Cleveland and Cyprus-Piños Altos [formerly known as Birchville (Lasky and Wootton 1933)] deposits occur in the Piños Altos district.

The Piños Altos Mountains are underlain by a faulted east-dipping Pennsylvanian-age sequence of quartzite and limestone (Ecology and Environment Inc. 1993, unpub. report). During the Laramide orogeny in the Late Cretaceous, compressional tectonics resulted in the emplacement of the Piños Altos granodiorite stock, and many diorite porphyry dikes and sills in contact with Pennsylvanian sediments (Paige 1910; North and McLemore 1986). This intrusion resulted in the formation of two types of deposits: (1) fissure filling in intrusive rocks, and (2) mineral replacement in limestone (Paige 1910). The Cyprus-Piños Altos deposit is located in the higher-temperature Cu-rich zone of alteration (McKnight and Fellows 1978) which contains both types of mineralization, and is classified as a Cu skarn. The Cleveland deposit is located in the lower-temperature Zn-Pb-Ag zone of alteration, consists of only mineral replacement bodies in limestone, and is classified as a Zn skarn (Bush 1915; North and McLemore 1986). In both deposits, the most common ore minerals were chalcopyrite, sphalerite and galena. Gold and silver occurred mainly in fissure fillings

in the Cyprus-Piños Altos deposit, and as by-products in the Cleveland deposit. Common gangue minerals in both deposits include quartz, calcite, garnet, magnetite, hematite, epidote, and diopside (North and McLemore 1986; Walder, Chavez 1995).
The limestone formations underlying the Cleveland mill and mill valley tributary are the Pennsylvanian-age Oswaldo and Colorado Formations. A northeast-trending west-dipping fault can be traced through the center of the main-tailings pile, parallel to the walls of the valley. The west pile overlies the Beartooth Quartzite and the east tailings overly the Oswaldo Limestone Formation. Downstream from the mill, the Little Walnut Creek streambed is underlain by the Colorado Limestone Formation. The Colorado Formation is the groundwater aquifer for the local domestic wells downstream (Ecology and Environment Inc. 1993, unpub. report).
The Cyprus-Piños Altos mine is located near the town of Piños Altos, on the eastern slope of the Piños Altos Mountains. The Cyprus-Piños Altos ore was transported to the town of Deming, New Mexico, for mill processing (Fig. 1). These tailings were deposited in a polyethylene-lined bermed impoundment. This impoundment is located in the flat arid Chihuahuan desert lowland. The Cleveland mine and mill site (Fig. 2) is located 3 km west of Piños Altos, in the less arid mountain woodland on the western flank of the Piños Altos Mountains.

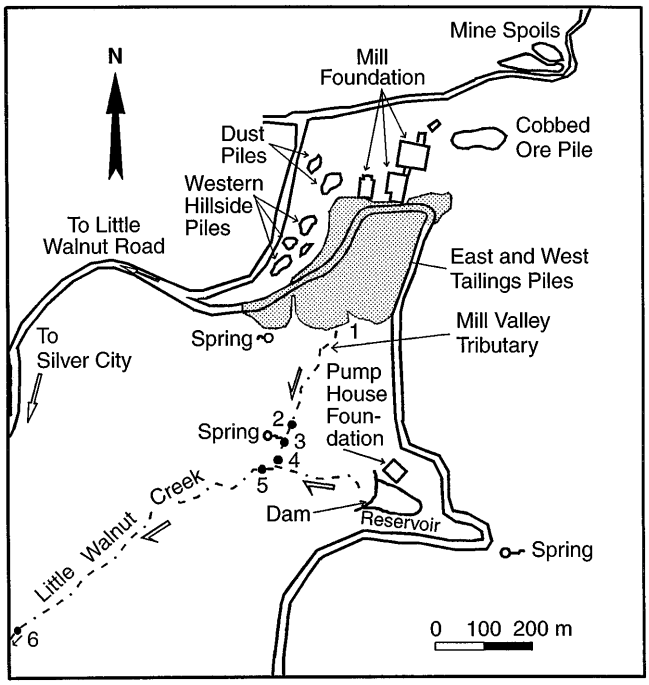

Fig. 2
CMT site map; *1–6* indicate streamwater sample sites (modified from Ecology and Environment, 1993, unpub. report)

Methodology

Sample collection

Samples of the tailings and the surrounding waters were collected at both sites in February 1995. Tailings samples were chosen according to differences in the grain size, water saturation, color, and cementation. At the Cyprus-Piños Altos tailings impoundment, a vertical sequence of 6 tailings samples (PAT003–PAT008) was collected at 15-cm-vertical intervals using a hand-held auger. Surface tailings also were collected, as was tailings pond water. Due to the unstable nature of much of the subaerial tailings material, sampling was restricted to a small region of the impoundment. At the Cleveland mill-tailings impoundment (Fig. 2), a sequence of 4 tailings samples (CMT001–CMT004) were taken from an erosional trench which exposed the tailings stratigraphy. Surface samples also were collected. Water samples were collected at various locations along the mill valley tributary which drains the tailings piles and which empties into Little Walnut Creek. Upstream from this confluence, Little Walnut Creek has been dammed to form a reservoir (Fig. 2).
Dry and slightly moist tailings samples were collected in plastic resealable bags. Moist and water-saturated tailings and stream-sediment samples were collected in 1-l Nalgene bottles. Water samples were filtered through 0.45-μ-pore filter paper in a magnetic holder and collected in a side-arm flask. The flask was rinsed with the first volume of filtrate, in order to "precontaminate" the flask. The second volume of filtrate was stored in 125-ml Nalgene bottles. At the time of collection, the temperature and the pH of the waters were measured using a pH/temperature meter. After filtering, the waters were acidified to a pH between 1.5 and 2 with concentrated nitric acid to prevent any dissolved metals from precipitating.

Sample preparation and analysis

At the University of Manitoba, water samples were filtered and immediately analyzed with a Liberty 2000 inductively-coupled plasma (ICP) emission spectrometer for dissolved metals. Tailings samples were dried in covered watch glasses. Once dry, 60 ml of each bulk tailings sample was crushed to a fine powder, using a tungsten-carbide crucible and ring grinder. The powdered samples were then mounted on glass slides by the acetone-slurry method for mineralogical analysis by x-ray diffraction (XRD), using a Philips x-ray generator with a fully-automated PW 1710 x-ray powder system. Diffractograms were entered into a computer and a mineralogical search was conducted using PEAKSEARCH Micro Powder-diffraction Search Match software (μPDSM) to identify the major crystalline phases present in the samples. The minimum number of reflections needed for identification of a mineral by XRD ranged from 4 to 9, depending on the intensity of the reflections and total number of reflections for a given pattern. Portions of the crushed samples (minimum of 2 g) were sent to Activation Laboratories in Ancaster, Ontario, for geochemical analysis. A total of 46 elements were analyzed in each sample using a combination of instrumental neutron-activation analysis (INAA)

and ICP methods. Sulfide (S), sulfate (SO_4) and carbonate (as evolved CO_2) were determined by Leco combustion, using an infrared detector. Structurally bound water (H_2O^+; Rollinson 1993) was determined by gravimetry. The geochemical results aided in the identification of mineral phases by limiting the XRD peak search to minerals and inorganic phases containing particular elements. Bulk samples were mounted on stubs and analyzed with a Stereoscan 120 (Cambridge Instruments) scanning-electron microscope (SEM) to characterize the surfaces of grains. Energy-dispersive x-ray (EDX) spectra were acquired for various grains and grain coatings to determine their chemical composition. Samples of bulk tailings also were impregnated with epoxy and made into polished thin sections. Highly cemented samples were cut perpendicular to the layering within the sample. Caution was taken during the slide preparation to prevent water contact with delicate secondary- and tertiary-mineral assemblages; oil-based products were used as cooling agents during cutting. Selected grains in thin sections were quantitatively analyzed using a electron microprobe.

Cyprus-Piños Altos mine tailings

Mineralogy

The CPAT tailings have a buff-grey color and are dominantly water-saturated, except near the effluent spouts where dry to slightly moist tailings form a broad cone. During processing, ore from the Cyprus-Piños Altos mine was crushed to a very fine-sand size where 65% of the grains are ≤ 125 μm in diameter and 100% of the grains are ≤ 1 mm in diameter. The primary sulfide-tailings mineralogy consists of pyrite, chalcopyrite, bornite, sphalerite, galena, and minor arsenopyrite (McKnight and Fellows 1978; Albert Arrey, pers. Comm. 1995). Gangue minerals include calcite, quartz, magnetite, grossular, andradite, and diopside (North and McLemore 1986). Of the primary-mineral assemblage, calcite, quartz, and pyrite are dominant, also making up the majority of the coarser grain-size fraction. Petrographic analysis of the tailings shows that these tailings are little altered, lacking any evidence of significant dissolution of primary minerals. A lime slurry was added to the tailings during processing to maintain a neutral to slightly alkaline pH. The alkaline nature of the tailings pond water is above the pH needed for the dissolution of calcite (Ptacek and Blowes 1994). The absence of calcite buffering reactions is supported by the presence of pristine calcite grains with angular grain boundaries (Fig. 3).

Secondary minerals are absent in these tailings. Tertiary minerals occur throughout the dried tailings samples, mostly as precipitates coating primary-mineral surfaces. The only tertiary mineral identified is gypsum, which occurs mainly as microscopic rosettes in fractures and corners of the grains, or as radiating clusters of crystals along grain edges (Fig. 4). Gypsum occasionally coats entire grains. Quaternary minerals have not been identified.

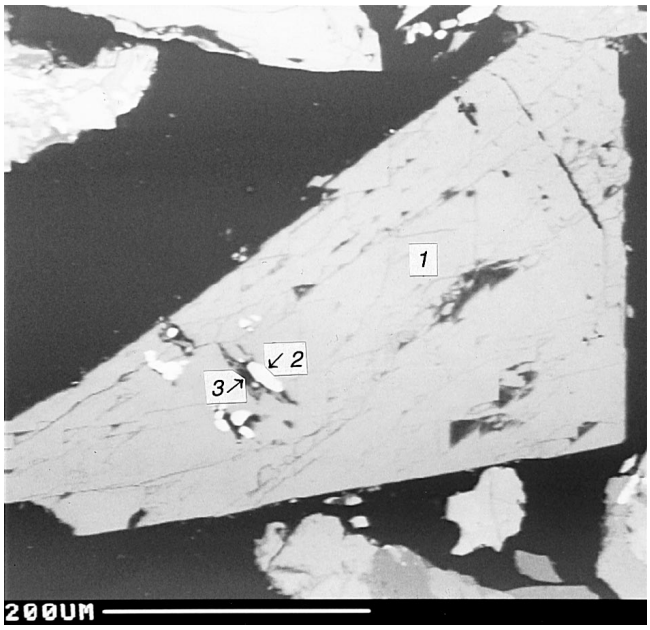

Fig. 3
Backscattered-electron (BSE) scanning-electron microscope (SEM) image of calcite in CPAT; (1) calcite, (2) gypsum, and (3) pyrite. The calcite has smooth cleavage edges, indicating that calcite dissolution is not occurring

Fig. 4
Secondary-electron (SE) image of tertiary gypsum on the surface of diopside

Geochemistry

Table 3 summarizes compositional data for tailings, ore, and concentrate for both CPAT and CMT. Sulfide S concentrations in the CPAT range from 1.10 to 2.44 wt.%. Sulfate contents range from below detection (<0.01 wt.%) to 0.95 wt.%. Structurally bound water content (H_2O^+) ranges from 0.75 wt.% to 1.84 weight per-

Table 3
Geochemical data for tailings, ore, and concentrate

Elements Units	Al wt.%	Ag ppm	Au ppb	As ppm	Ca wt.%	Cd ppm	Cu ppm	Fe wt.%	K wt.%	Na wt.%	Pb ppm	Sb ppm	Zn ppm	S wt.%	SO_4 wt.%	CO_2 wt.%	H_2O^+ wt.%
PAT001	2.29	8.3	215	110	16.8	4.1	2228	12.1	0.33	0.09	314	50	560.5	1.35	0.03	7.25	0.91
PAT002	2.34	15.4	430	83	16.985	7.9	9702	12.8	0.25	0.05	615	38	1050	2.44	0	6.36	0.76
PAT003	2.25	15.8	398	91	17.42	7.6	6931	15.1	0.16	0.04	948	36	1060.5	2.49	0	5.31	0.86
PAT004	2.61	9.9	430	60	17.105	4.0	4245	12.5	0.24	0.09	278	19	560	1.6	0.897	4.9	0.77
PAT005	2.49	6.1	252	51	19.265	2.5	2363	12.7	0.27	0.08	167	10	437	1.07	0.428	5.89	0.83
PAT006	2.36	8.4	388	42	18.55	3.5	2871	12.4	0.29	0.08	137	9	547.5	1.1	0	6.66	0.77
PAT007	2.55	9.35	330	47	18.71	3.4	2683	10.9	0.32	0.1	124	9.9	534	1.29	0.0329	7.98	0.88
PAT008	2.62	9.8	828	43	18.815	2.9	2056	11.1	0.32	0.09	111	5.7	500	1.2	0.508	8.45	0.75
PAT009	2.42	6.75	149	96	16.65	2.2	1113	10.3	0.49	0.11	231	41	437.5	1.14	0.945	11.1	1.84
PAT010	2.29	1.25	90	70	18.51	1.9	715	10.4	0.34	0.08	265	30	197.5	0.921	1.56	8.64	1.30
PAT011	2.57	6.3	287	57	17.84	3.9	2651	11.8	0.3	0.11	167	24	590	1.26	0.179	5.75	1.13
PAT012[1]	0.34	161.05	2280	290	2.19	78.7	99999	24	0.03	0.01	1444	220	8712	24.4	0	0.059	2.56
CMT001	0.49	34.05	18	93	10.12	2.2	701	7.08	0.24	0.01	488	14	451	10.1	29.6	0.011	9.56
CMT002	0.52	32.3	8	85	7.71	3.8	979	9.95	0.22	0.01	408	14	821	13.9	30	0.015	9.55
CMT003	0.5	41.9	170	72	8.43	4.9	1259	9.25	0.22	0.02	535	17	1505.5	13.4	31.8	0.051	10.47
CMT004	0.51	33.7	12	66	6.4	195.5	5442	13.00	0.17	0.01	412	14	41212	16.8	30.3	2.29	8.24
CMT005	0.59	139.7	22	3.7	9.72	1.4	2308	2.06	0.33	0.02	1533	41	201.5	10.7	29.5	0	10.43
CMT006	0.59	51.6	0	120	6.21	76.9	16173	14.7	0.14	0	427	19	22356.5	15.2	0	0.359	5.69
CMT007	0.68	45.8	7	86	9.155	36.4	31738	12.6	0.08	0	378	16	7777	17.1	32.4	0.417	10.02
CMT008	0.33	61.6	327	31	0.75	11.7	4231	32.5	0.04	0	601	19	15600	15.1	25.9	0	10.46
CMT009	0.37	80.75	15	42	1.405	11.2	1374	31.3	0.07	0.01	888	24	14475.5	14.0	4.78	0.018	5.82
CMT010	0.22	7.1	0	36	0.155	38	2315	20.1	0.01	0	133	2.9	16473	NA	NA	NA	NA
CMT011	0.36	61.4	40	44	1.6	3.5	933	36.8	0.04	0	531	15	12428	12.8	23.7	0.007	9.13
CMT012	0.84	25.45	9	190	5.34	11	741	10.1	0.32	0.08	406	17	4068.5	5.81	15.5	0.011	8.56
CMT013	0.41	56.7	187	46	3.2	1.9	1202	36.2	0.1	0.01	718	18	10720	4.51	11.1	1.38	5.59
CMT-1[2]	0.12	58.2	0	98	0.14	823.5	12666	21.2	0.02	0	360	13	141000	24.0	13.5	1.35	0.40

NA not available
[1] ore concentrate
[2] ore sample; all other samples are tailings

cent. Carbonate values range from 4.9 to 11.1 weight percent. Tailings metal concentrations range from 715 to 9702 ppm for Cu, 197.5 to 1060.5 ppm for Zn, 111 to 948 ppm for Pb, 6.1 to 15.8 ppm for Ag, and 90 to 823 ppb for Au.

A vertical sequence of 6 tailings samples (PAT003–PAT008) was collected at 15-cm intervals. The tailings in the section range in grain size from coarse to medium sand; they are grey-brown to brown in color, and are progressively more water-saturated with depth through the section. Geochemical depth profiles are shown in Fig. 5. Similar trends can be observed for sulfide S, Ag, Cd, Cu, As, Pb, Sb, Fe and Zn, where the upper most interval is enriched in these elements and concentrations decrease with depth. In contrast, the CO_2 depth profile shows the reverse trend, increasing with depth. The amounts of structurally bound water (H_2O^+) approach detection limits throughout the section. Geochemical variation diagrams for metals in the CPAT are shown in Fig. 6. For the metal species plotted, positive linear correlations exist.

Pond-water chemistry

At the time of sampling, water in the CPAT tailings pond was neutral to slightly alkaline (pH of 7–8.27). Water in the impoundment consists mainly of mill-derived effluents, rather than rainwater. Dissolved metal concentrations are as follows: 0.03 ppm As, 0.01 ppm Fe, 0.04 ppm Pb, 51 ppm S, 0.01 ppm Se, and 0.07 ppm Zn; Ag, Cd, Cu, and Hg concentrations are all below detection.

Cleveland mill tailings

Mineralogy

The east pile of the CMT has a dark brown color, while the west pile has a dominantly rusty orange-yellow color. The mineralogy of each side reflects the orebody zone that was being mined at that time. No tailings from other mine sites were deposited at this site (U.S. EPA 1993, unpub. report). The primary-mineral assemblage of these tailings has been almost completely dissolved or oxidized; a small fraction of primary minerals still remain. The primary sulfide minerals include pyrite, sphalerite, chalcopyrite, and minor galena, arsenopyrite, and tetrahedrite; gangue minerals include quartz, calcite, grossular, andradite magnetite, diopside, and minor hematite (Paige 1910; Walder and others 1994). While it has not been observed in our samples, McKnight and Fellows (1978) have documented tennantite in the Cyprus-Piños Altos deposit. This mineral also may be present in the CMT, and is of environmental concern because it contains As.

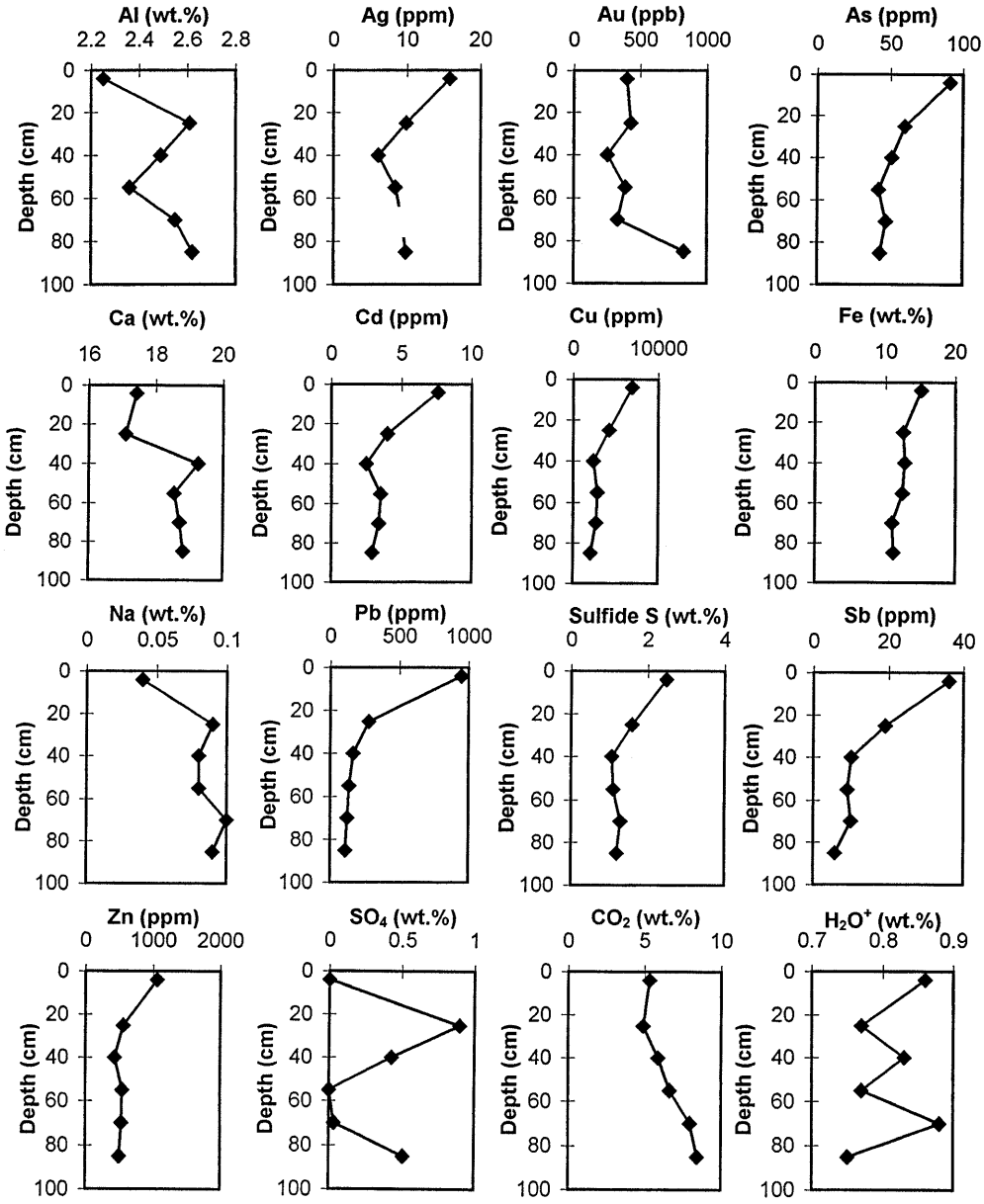

Fig. 5
Geochemical depth profiles of a vertical section through the upper 1 m of the Cyprus-Piños Altos tailings

The most abundant primary minerals which still occur in the tailings are pyrite and quartz; sphalerite and chalcopyrite also are present, but in minor quantities. Most calcite has been dissolved as a result of buffering reactions; however, some is still present at the extreme base of the east tailings. Most primary minerals, particularly sulfide minerals, have been either completely or partially dissolved or replaced, resulting in skeletal or zoned grains. Pyrite and sphalerite grains show well-developed complex alteration patterns. Highly fractured sulfide grains have a skeletal appearance, where there is abundant alteration product making up the grain. Less-fractured sulfide grains have a zoned appearance, with a core of primary sulfide and a series of alteration rims. The innermost zone of altered pyrite commonly consists of specular hematite and Fe-oxyhydrosulfates (Fig. 7). The middle zone commonly consists of Zn-bearing Fe-oxyhydrosulfates and/or -sulfates. The outermost zone consists of gypsum and jarosite. The oxidation of sphalerite also results in a layered rind of secondary minerals (Fig. 8). The innermost zone consists of native sulfur, and the outermost rim consists of a hydrous Fe-sulfate. The oxidation products of chalcopyrite are similar to those of pyrite, except that there are Cu and Zn impurities in the Fe-sulfates. Primary quartz commonly is coated with layers of Zn-bearing hydrous or nonhydrous Fe-sulfates, secondary and tertiary gypsum, and jarosite (Fig. 7). Grains commonly are cemented to surrounding particles by secondary and tertiary gypsum. Secondary minerals are abundant in the tailings, giving them their distinct rusty color. Microscopic examination of the secondary minerals revealed distinct colors of material. This feature along with EDX spectra and XRD has been used to develop a "color index" which identifies the dominant mineral in each

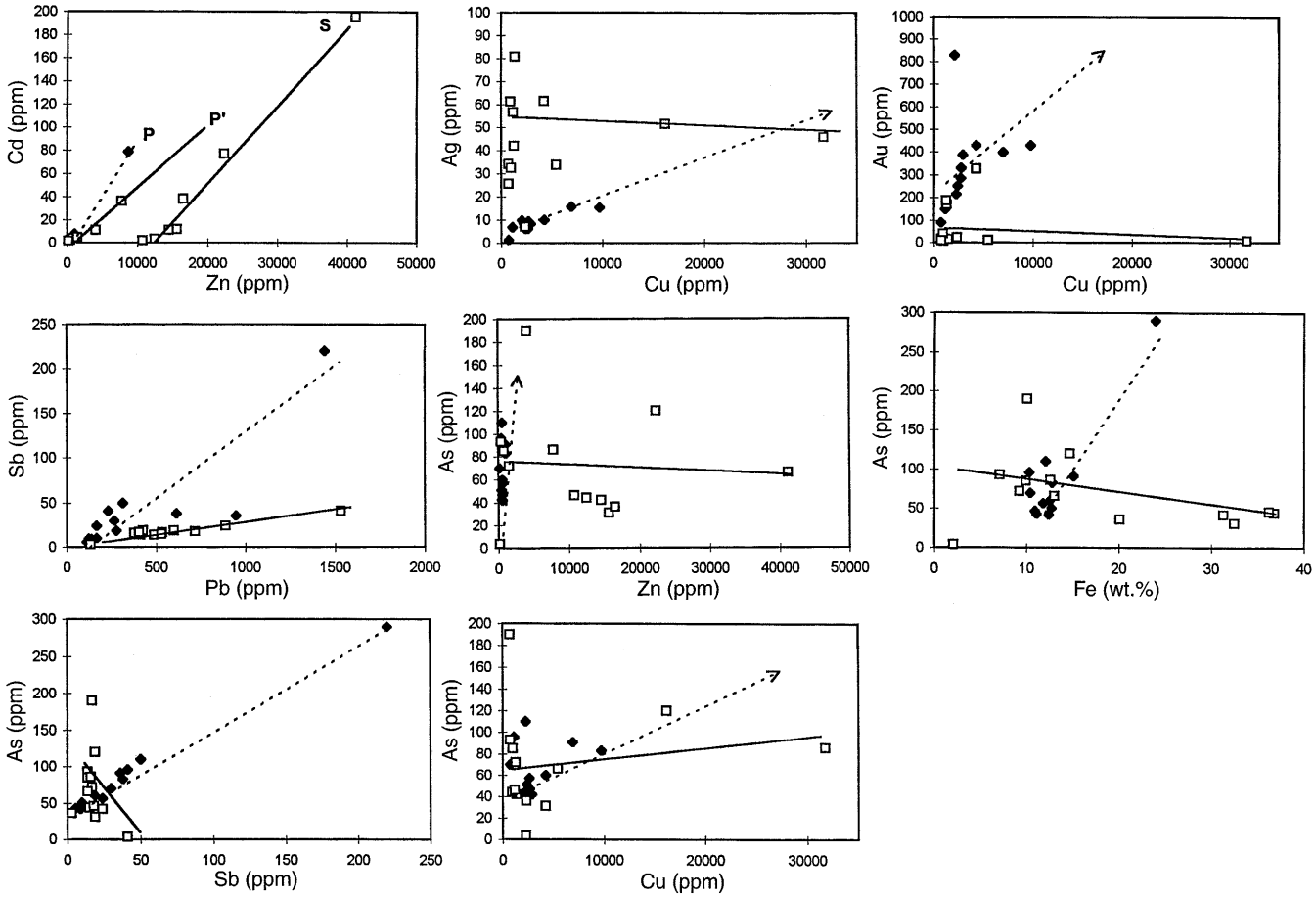

Fig. 6
Variation diagrams comparing CMT and CPAT geochemical results. *Solid line* and □ indicate CMT samples; *dashed lines* and ♦ indicate CPAT samples. *P* and *P'* indicate primary trends for CPAT and CMT, respectively, while *S* indicates a secondary trend for CMT. *Arrows* point to the value for ore concentrate from the Cyprus-Piños Altos mine. See Table 3 for ore and concentrate compositions. Correlation coefficients (*r*) for CPAT and CMT, respectively, are as follows: **a** 1.00 (P), 0.971 (P′), 0.993 (S); **b** 0.999, –0.044; **c** 0.927, –0.194; **d** 0.86, 0.953; **e** 0.95, –0.096; **f** 0.904, -0359; **g** 0.994, –0.287; and **h** 0.947, 0.177

sample. Five color categories have been defined: metallic grey, yellowish-brown (Munsell hue 5YR 4/6), bright orange (approximately Munsell hue 5YR 6/8), reddish-brown (Munsell hue 7.5YR 3/6), bright yellow (Munsell hue 2.5YR 8/8) and straw yellow (Munsell hue 10YR 8/6; Jambor 1994). The dominant phases making up the samples corresponding to this index are specular hematite (Fe_2O_3), goethite (α-FeOOH), lepidocrocite (γ-FeOOH), ferrihydrite ($5Fe_2O_3 \cdot 9H_2O$), schwertmannite [$Fe_8O_8(OH)_6SO_4$], and jarosite [$KFe_3(OH)_6(SO_4)_2$], respectively. The presence of an Fe-oxide with the formula Fe_2O_3, in direct contact with altered pyrite was confirmed by EMP analysis; however, the exact phase (hematite versus maghemite) is uncertain. It likely is hematite, as this has been found to be a product of pyrite oxidation in coal wastes; maghemite is a product of magnetite alteration (Jambor 1994). Gypsum and various Fe-oxyhydroxides and -sulfates also make up a minor portion of the secondary phases. These phases result from the oxidation of sulfides. They coat the remaining primary minerals and differentially cement them. At various intervals throughout the tailings, these secondary minerals have cemented the tailings to form hardpans and encrusted layers. Secondary gypsum occurs throughout as a cementing mineral, and as massive irregular clumps coated with a thin layer of Fe oxyhydroxides. Secondary gypsum commonly has traces of Fe and Zn, likely as inclusions. Jarosite occurs as small clusters of acicular crystals (~5 μm long), or as continuous coatings on grains as bands of fine feathery radiating crystals (Fig. 9).

Most of the samples were dry when collected; however, precipitation of minerals from residual pore waters formed tertiary hydrous sulfates in some samples. The most abundant tertiary mineral is gypsum. Tertiary gypsum does not contain impurities (Fe and Zn) as observed in secondary gypsum; it occurs as small white blooms forming radiating clusters of acicular crystals, or clumps of small stubby crystals in cracks and corners. Melanterite ($FeSO_4 \cdot 7H_2O$) was identified in the east tailings; it occurs as clear pale-blue filiform crystals, 0.1–1 cm in length. Rozenite is the only quaternary mineral identified.

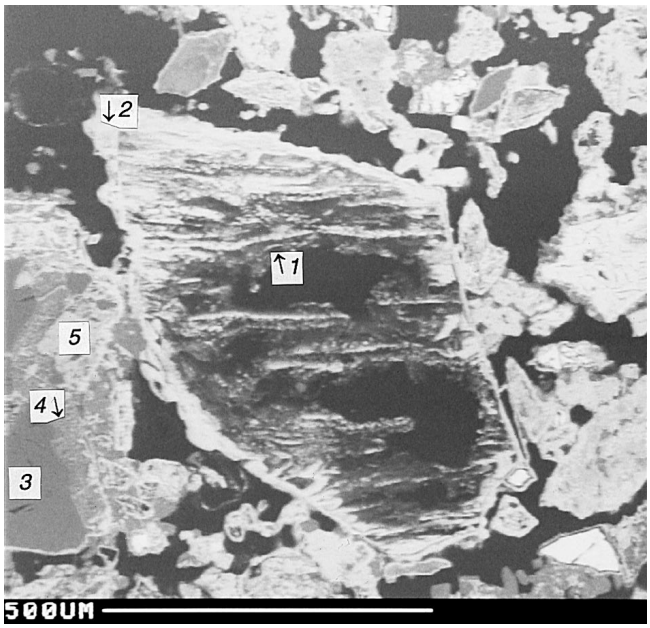

Fig. 7
BSE image of an extensively altered pyrite: *1* Fe-depleted grain with a well developed *2* three layer rim of hematite, Zn-bearing Fe oxyhydrosulfate and thin rim of tertiary gypsum. The brighter regions within the grain represent remnant pyrite; the dark center is a cavity caused by grain plucking during slide preparation. *3* Quartz grain with a complex coating of precipitates; *4* mainly Fe-rich gypsum; *5* Zn-bearing Fe oxyhydrosulfate

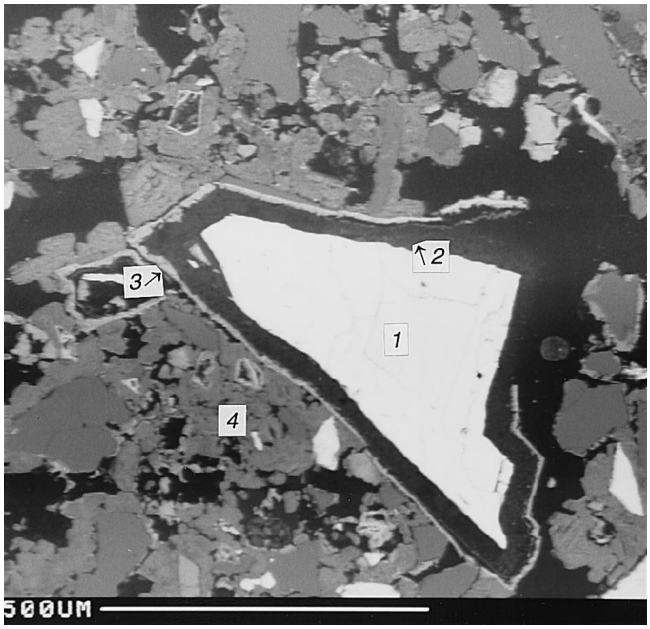

Fig. 8
BSE image of *1* altered sphalerite with *2* an inner alteration rim of native S and *3* an outer rim of possibly hydrous Fe-sulfate; *4* tertiary gypsum crystals surround the altered grain

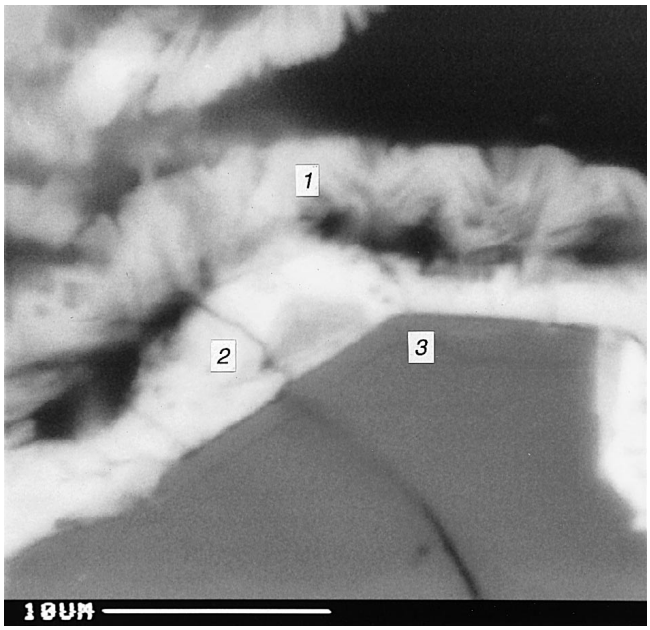

Fig. 9
BSE image of *1* feathery secondary jarosite and *2* Zn-bearing Fe-hydrous sulfate coating *3* quartz

Geochemistry

Metal and complex ion concentrations vary greatly in these tailings: 0 (below detection)–32.4 wt.% sulfide S, 4.51–17.1 wt.% SO_4, 0–2.29 wt.% CO_2, 701–31738 ppm Cu, 451–31738 ppm Cu, 451–41212 ppm Zn, 133–1533 ppm Pb, 7.1–139.7 Ag, and 0–347 ppb Au. Ore sample (CMO-1) metal concentrations fall below the highest concentration in the tailings, with the exception of Zn and sulfide S (Table 3). Lower concentrations of As were measured in this study (3.7–190 ppm) than reported by previous workers [eg., 276 ppm reported by Shantz (1993, unpub. report), 366 ppm reported by Ecology and Environment (1993, unpub. report)]. The highest levels observed in this study come from a stream-sediment sample downstream from the CMT in the mill valley tributary. Arsenic concentrations in the streamwater were below detection limits (<0.003 ppm).

Samples were collected on the surface of the tailings and from a vertical section through the upper 50 cm of the west tailings (Table 4). The distribution of elements through the vertical profile are shown in Fig. 10. Several different geochemical trends are apparent in the depth profiles. The most common trend shows a gradual increase in concentration with depth and a pronounced increase in concentration in the hardpan (CMT004). Elements showing this trend include Cd, Cu, Zn, and Fe. Elements that show an increase above the hardpan (CMT003), include Ag, Au, Na, Sb, and Pb. Arsenic has a unique profile, with the concentration decreasing with depth and is lowest in the hardpan. Sulfide S concentrations gradually increase with depth. The sulfate profile varies little with depth with the exception of a slight increase above the hardpan. A similar trend is observed for

Table 4
CMT sample descriptions for depth profiles

Sample #	Color (Munsell hue)	Texture	Depth (cm)
CMT001	rust orange (10YR 5/8)	mostly loose grains, slightly cemented	0–10
CMT002	yellow-green with dark rusty orange base (10YR 6/6)	loose with small cemented grains	10–13
CMT003	rusty brown-orange (approx. 7.5 YR 5/6)	loose with small cemented grains	13–46
CMT004	dark grey-brown with unoxidized pyrite and silicates (7.5 YR 3/2 to 5/6)	highly cemented with secondary minerals (hardpan)	46–50

structurally bound water. The carbonate depth profile is identical to that shown by Cd, Cu, Zn and Fe. Geochemical variation diagrams for CMT show a variety of element relationships (Fig. 6). Positive correlations exist between Cd and Zn, Sb and Pb, and As and Cu. Negative, poorly defined correlations exist between Au and Cu, Ag and Cu, As and Zn, As and Fe, and As and Sb.

Stream water chemistry

Figure 2 shows dissolved-metal concentrations of water samples collected at varying distances downstream from the Cleveland mill tailings. Immediately below the tailings, the pH of the stream water was 2.3 and metal concentrations were high (Fig. 11). At a distance of 300 m downstream, water from an ephemeral spring mixed with the acidic drainage of the mill valley tributary. The spring water had a neutral pH and had formed a small travertine deposit on the west slope just above the acidic stream. The pH of the stream increased slightly up to 2.5 immediately below the confluence with the spring, and dissolved-metal concentrations decreased. At a distance of 3.5 km downstream, pH increased to 7.27 and metal concentrations fell below detection limits.

Discussion

There is little evidence of alteration of the CPAT, and thus trends in variations diagrams (Fig. 6) reflect primary geochemical coherences. For example, Cd shows a positive linear correlation ($r = 1.00$) with Zn, indicating that Cd is hosted by sphalerite (Fig. 6a). Similarly, Ag correlates positively with Cu, as it is mainly hosted by or associated with chalcopyrite (Fig. 6b). Gold also correlates positively with Cu (Fig. 6c), although the trend is less well defined than that for Ag versus Cu. The positive correlation between Sb and Pb suggest that galena is the main host of Sb, although sulfosalts (e.g., boulangerite) also may host Sb. While sulfosalts have not been observed in our ore or tailings samples from either site, the positive correlations between As and Sb and between As and Cu (Fig. 6g and h) suggests that both are hosted by fahlore group minerals (tetrahedrite-tennantite). The main host of As in the CPAT is likely arsenopyrite, as suggested by the positive correlation between As and Fe (Fig. 6f). We have not observed arsenopyrite in ore or tailings, but it has been reported in the Cleveland deposit by other workers (McKnight and Fellows 1978; North and McLemore 1986), and we have observed it in the CMT.

Unlike the CPAT, there is abundant evidence of chemical weathering of the CMT. Thus, variation diagrams for the CMT must be interpreted with regard to both primary mineralogy and secondary processes. Because of the similarity in mineralogy of the two deposits, compositional relationships in the CPAT may be used as an indication of those in the CMT prior to the onset of chemical weathering. Trends in variation diagrams for CMT reflect the superposition of secondary assemblages on primary assemblages. The plot of Cd versus Zn shows a single linear relationship for CPAT and two linear relations for CMT, one of which converges with the CPAT assemblage (Fig. 6a). Trend 'P' reflects a primary signature in the CPAT, with Zn and Cd both occupying sphalerite. Trend 'P'' is interpreted as a primary trend for the CMT. The slightly lower slope than that shown by trend P is likely due to lower Cd content of sphalerite in the Cleveland deposit than that of sphalerite in the Cyprus-Piños Altos deposit. Trend 'S' may represent a secondary relationship developing under conditions where following oxidation of sphalerite, Zn was less mobile but Cd was strongly leached from the tailings.

Positive correlations in the CPAT of As versus Fe (Fig. 6f) and As versus Cu (Fig. 6h) suggest that As is present in arsenopyrite as well as tetrahedrite-tennantite. The positive correlation between As and Sb in the CPAT (Fig. 6g) also suggests that As may be hosted by tetrahedrite-tennantite. As Zn can substitute for Cu in fahlore group minerals, the positive correlation between As and Zn in the CPAT (Fig. 6e) also may reflect the presence of tetrahedrite-tennantite. The negative correlations between As and Zn, Fe, and Sb in the CMT suggest that tetrahedrite-tennantite has broken down and different relative mobilities have separated these elements during chemical weathering. The positive correlation between As and Cu in the CMT suggests that As may be present in secondary Cu-sulfides rather than fahlore group minerals, although secondary sulfides have not yet been observed. The scattering of the CMT data suggests that the secondary mobility of As has had a complex history. A bulk ore sample from the Cleveland mine that contains sphalerite, chalcopyrite, and pyrite but no observable arsenopyrite contained 98 ppm As. EMP analysis of sphalerite, pyrite, and chalcopyrite revealed that detected concentrations of As are at or below detection limits. Further analysis by proton-induced x-ray emission (PIXE), which has lower detection limits then EMP, will be done to verify the siting of As and other toxic elements (eg., Cd, Sb).

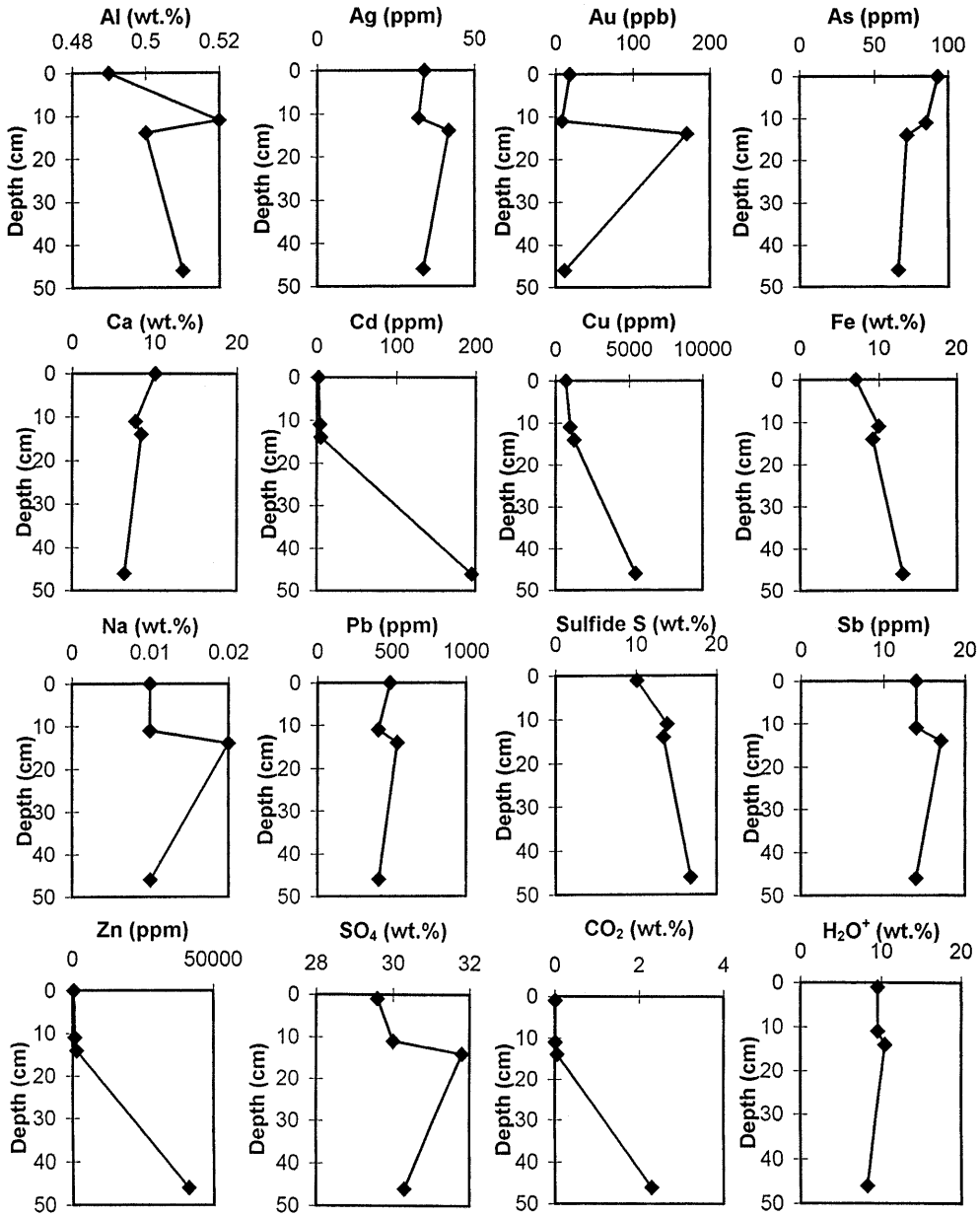

Fig. 10
Geochemical depth profiles of a section through the upper 50 cm of the CMT; top of hardpan is at 46 cm

As the CPAT show little evidence of alteration, the geochemical depth profiles directly reflect the primary mineralogy of the tailings samples (Fig. 5). The elevated S, Ag, Cd, Cu, As, Pb, Sb, and Zn in the upper 15 cm of the vertical section reflect the relative sulfide enrichment in this upper interval. Variations in element concentrations may be a function of: (1) the grade of ore zone being mined during a given period, (2) efficiency of extraction processes, and (3) mineral partitioning during deposition (resulting from grain-size sorting). Sieve analyses were conducted on all the samples from the section. Samples showed little grain-size variation with depth, suggesting that mineral partitioning during deposition is not the cause for the variations. Unlike those for the elements above, concentrations of Ca, Al, and CO_2 (carbonate) are low at the surface, but increase with depth. This relationship may be directly related to the reactivity of the sulfide and gangue minerals at the surface of the tailings, or to the relative dilution of gangue minerals by sulfides if the sulfide content is high at the surface.

The Cyprus-Piños Altos tailings have undergone very little, if any, mineralogical and geochemical changes since their deposition. The addition of lime to the tailings has maintained a neutral pH, thus preventing sulfide oxidation, as well as the dissolution of gangue minerals such as calcite. However, the precipitation of tertiary gypsum from pore water indicates that the tailings have not been completely unreactive. The relative reactivity of sulfides in a tailings environment is pyrrhotite>sphalerite-galena >pyrite-arsenopyrite>chalcopyrite>magnetite (Jambor 1994). Pyrrhotite is absent in the CPAT; thus, sphalerite and galena are the most reactive sulfide mineral in the

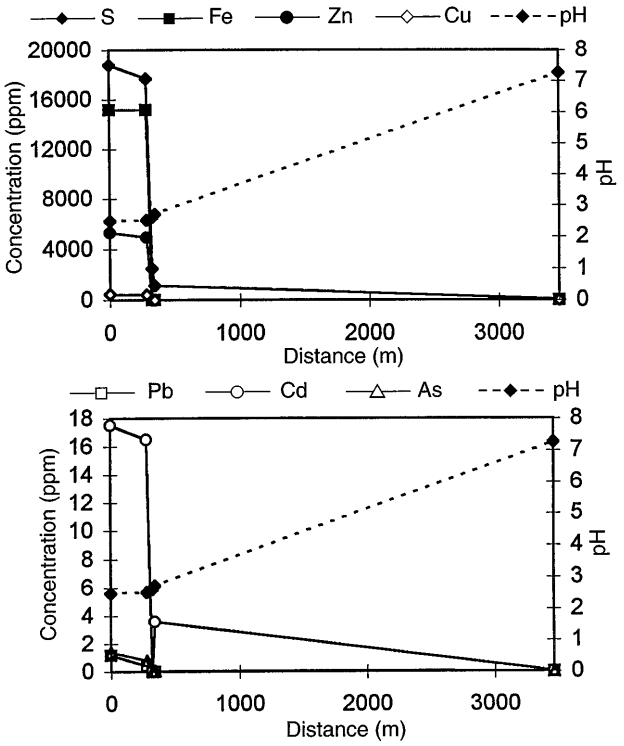

Fig. 11
Dissolved metal concentration and pH in streamwaters as a function of distance downstream from CMT

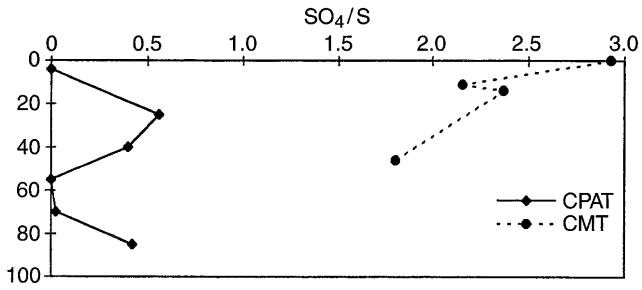

Fig. 12
Depth profile of SO_4/sulfide S ratio in CPAT and CMT

impoundment. Electron-microprobe analysis of the sphalerite in the CPAT revealed Fe concentrations as high as 10.76 wt.%. Such elevated Fe contents in sphalerite result in tetrahedral distortions of the crystal structure (Shadlum and Turpeko 1970), thus increasing its surface reactivity with the pore water. The low sulfate/sulfide ratio (Fig. 12) in the bulk tailings suggests that although most of the total sulfur is in the sulfide state, a small fraction has been oxidized to sulfate. Although the dissolved concentrations of Zn and S in the pond water are relatively low (0.07 ppm and 51 ppm, respectively), the concentrations of other metals are even lower. This suggests that sphalerite is the most likely source of SO_4^{2-}, and lime added during processing is the source of Ca^{2+}. During drying of the tailings in the lab, concentrations of Ca^{2+} and SO_4^{2-} in the pore water increases (as the volume of water decreases) until gypsum saturation occurs and gypsum precipitates.

Geochemical depth profiles of the vertical section of the CMT reflect a relationship between chemistry and environmental conditions. The hardpan, located at a depth of 46 cm, is the lowermost zone of a 50-cm-thick section sampled, and represents the local zone of acid neutralization and chemical precipitation (Blowes 1990; McGregor 1994). This zone is highly cemented and has elevated concentrations of metals. The three zones above this hardpan represent the sulfide-oxidation and acid-generation zones. These upper three levels contain completely to partly oxidized sulfides and are mainly composed of secondary minerals; McGregor (1994) found these zones to have high acid generation and high dissolved metal concentrations in pore waters. In tailings environments, downward moving water in the tailings becomes acidic until it reaches a zone where the acid is neutralized, and where a high proportion of gangue minerals and minimally altered sulfides remain. The SO_4/S ratio for CMT (Fig. 12) shows a decrease in sulfate with depth corresponding with an increase in sulfide S, as expected by the transition from oxidizing to reducing zones. Acid neutralization caused by carbonate dissolution decreases the solubility of dissolved elements, thereby causing these elements to precipitate (usually as secondary carbonates, oxides, and oxyhydroxides). Such a trend is clearly visible in the geochemical depth profiles for many elements in the CMT, including Cd, Cu, Fe, and Zn, as well as for CO_2(Fig. 10). These metals require acidic conditions to be transported from their source; increasing pH causes precipitation in the hardpan layer. The hardpan layer at CMT contains abundant unaltered sulfide and gangue minerals. The presence of sulfides in the hardpan is reflected in the increased amount of sulfide S in this zone (Fig. 10). The high metal concentrations in the hardpan are the result of both preservation of primary sulfides and precipitation of secondary oxides and carbonates; no secondary sulfides have been observed.

Elements such as Ag, Au, Pb, and Sb tend to concentrate in the layer above the hardpan. These elements are reactive metals that form highly insoluble complexes with sulfate. As the percolating waters approached the hardpan, the pH increased slightly. This increase was enough to cause these highly insoluble metal-sulfate complexes to precipitate. This sulfate precipitation is also evidenced by the slight increase above the hardpan in the sulfate depth profile (Fig. 10). The same trend occurs in the profile for structurally bound water, suggesting that hydrated secondary minerals are most abundant above the hardpan. The concentration of Na also increases above the hardpan (Fig. 10); XRD results indicate that this is a zone of mass precipitation of natrojarosite [$Na, Fe_3(SO_4)_2(OH)_6$]. In contrast to geochemical profiles for base and precious metals, profiles for As, Ca, and K exhibit a gradual decrease in metal concentrations with depth. At the hardpan layer, jarosite, the primary K-bearing secondary mi-

neral, becomes slightly undersaturated in the pore water, causing it to partly dissolve. This same trend has been observed at the Copper Cliff tailings site in Sudbury, Ontario (McGregor 1994). Due to the high mobility of Ca under most conditions (Thornton 1983), the decrease in concentration with depth is unusual. This trend may be due to the mobility restrictions of a Ca-bearing complex, evaporation of Ca-rich pore waters near the surface, evaporative pumping, or primary-mineral distributions. In contrast, As has a moderate mobility under most conditions, but is immobile under reducing conditions (Thornton 1983); thus, a depth profile trend opposite of that observed would be expected. The distribution of As throughout the tailings may therefore be a function of the restricted mobility of an As-bearing complex, preferential uptake into a secondary phase, or primary-mineral distribution.

In the CMT, oxidation of sulfides resulted in the generation of acidic solutions and subsequent dissolution of gangue minerals, particularly calcite. The alteration rims on sulfides represent the effects of diffusion-limited alteration mechanisms which operated during the oxidation cycle described above. There is evidence for two distinct diffusion processes in the CMT: (1) outward diffusion of Fe, leaving a S-rich core or rim; and (2) outward diffusion of S, leaving an Fe-rich core or rim. The first process occurs most commonly in sphalerite, where native sulfur rims cover the remaining sphalerite core (Fig. 8). The second process occurs most commonly in pyrite, where a reactive Fe-rich rim is left behind; this rim reacts with the air and pore water to produce specular hematite (Fig. 7). All sulfides have multilayer rims, surrounding an unaltered core. Generally, the innermost layer is the diffusion-limited rim.

Although gypsum is the most common tertiary mineral in tailings, it is also present as a minor secondary mineral in the CMT. Evidence supporting a secondary origin is the occurrence of gypsum beneath layers of secondary Fe-oxyhydroxides and -oxyhydrosulfates. Secondary gypsum often contains small amounts of Fe, Zn, or Cu impurities, and has a massive crystal habit. Tertiary gypsum lacks impurities and forms stubby subhedral to euhedral crystals in the matrix, or radiating clusters on mineral surfaces. The Fe-oxyhydroxides and -oxyhydrosulfates and secondary gypsum are formed by wet/dry cycles which resulted in the occurrence of desiccation cracks in precipitates on grain surfaces. Wet/dry cycles also affect the surface of the tailings pile. During a trip to the CMT in November 1996, we observed white precipitates (mainly gypsum) covering the surface of the tailings. Our visit followed an extended period of dry weather. When samples were collected in Feburary 1995, the surface of the tailings was relatively free of efflorescent sulfates, because there had been abundant flushing of the tailings during early snow melt. Thus, gypsum layers coating individual grains are associated with periods of drying, when pore waters become saturated with respect to gypsum through water loss. In contrast, layers of Fe-oxyhydroxides and -oxyhydrosulfates are associated with wet periods when oxidative dissolution of sulfides increases the amount of dissolved Fe in pore waters.

Metal concentrations in stream water decrease with distance downstream from the CMT (Fig. 11). At the location where the acidic drainage mixed with the neutral springwater, the metal concentrations decreased significantly. This decrease was due in part to dilution, but also to co-precipitation and sorption of metals by secondary phases in the streambed, mainly Fe-oxyhydrosulfates and oxyhydroxides. The extensive precipitation of Fe minerals resulted in rusty coloration of the streambed below the tailings pile. The slight increase in pH and addition of dissolved carbonate at this location changed the water chemistry enough so it could no longer support the load of dissolved metals. Further downstream, the dissolved metal concentrations decreased until they were below detection limits. Low concentrations of Pb throughout the stream result from the precipitation of plumbojarosite ($Pb\ Fe_3\ (OH)_6\ (SO_4)_2$), and highly insoluble $PbSO_4$ in the tailings. Lead concentrations in the tailings are as much as two orders of magnitude *higher* than Cd concentrations, but Pb concentrations in the stream were up to one order of magnitude *lower* than Cd concentrations. This relationship indicates that Cd is easily mobilized out of the tailings. Zn also is highly mobile, due to relatively high solubility of $ZnSO_4$.

Conclusions

The Cyprus-Piños Altos and the Cleveland deposits had similar primary mineralogical assemblages and geochemical signatures. Because of differences in style of deposition and time since deposition of the tailings, present metal-residence sites differ substantially. However, the CPAT may be viewed as an analogue for the CMT early in its weathering history.

The CMT show chemical precipitation of metals in the hardpan layers, thus trapping many potentially toxic metals from further mobilization into the local environment. Metals that are not concentrated in the hardpans tend to be distributed throughout the tailings. This is a function of either primary mineralogical distribution, restricted mobility of a complex, or preferential uptake into a secondary phase. Preferential uptake is the dominant factor in the CMT, due to its advanced state of weathering; primary-mineral distribution is the dominant factor controlling metal distribution in the CPAT.

Our results indicate that mechanical transport of sediment downstream is an important mechanism in mobilizing of As from the tailings; however, chemical transport appears minimal. Zinc and Cd concentrations are moderately high in the streamwater, indicating that they are mobilized both within and outside of the tailings environment by chemical and mechanical transport mechanisms. Zinc and Cd are therefore of great concern when evaluating the toxicity of tailings and its effect on local acidic drainage. Low mobility of Pb within the tailings

and low concentrations of Pb in acidic drainage indicate that this element may pose less of a threat to the environment than other, more mobile, toxic trace elements (e.g., Cd) that are present in lower concentrations in tailings. An understanding of the relative mobilities of such toxic metals in different environments is therefore necessary when predicting or evaluating the impact of tailings on water quality.

Acknowledgments We wish to thank the following people: Don Lillie, Candy Ross and Dean Davis from the Mining Remedial Recovery Group for logistical assistance; Cyprus-Piños Altos Corporation for access to the Deming tailings impoundment; Albert Arrey, formerly of Cyprus-Piños Altos Corporation, and Jim Stimac, formerly of Los Alamos National Laboratory, for assistance with sampling; Fraser Goff of Los Alamos National Laboratory for the loan of sampling equipment. At the University of Manitoba, we are grateful to Sergio Mejia for assistance with SEM analysis, and Neil Ball and Mark Cooper for assistance with XRD analysis. The manuscript benefitted from thorough and constructive reviews by Virgil Lueth and Virginia McLemore. This research was supported by grants from the University of Manitoba and National Science and Engineering Research Council awarded to A.C.L.L.

References

Anderson EC (1957) The metal resources of New Mexico and their economic features through 1954, State Bureau of Mines and Mineral Resources Bulletin 39, US Government Printing Office, Washington, DC

Blowes DW (1990) The geochemistry, hydrology and mineralogy of decommissioned sulfide tailings: a comparative study. Ph.D. Thesis, University of Waterloo, Waterloo, Ontario

Bush FV (1915) Mining in the Piños Altos District of New Mexico. Min World Eng 42:165–168

Jambor JL (1994) Mineralogy of sulfide-rich tailings and their oxidation products. In: Environmental geochemistry of sulfide mine-wastes, MAC short course, pp 59–012

Lasky SG, Wootton TL (1933) Metal resources of New Mexico. N M Bur Mines Miner Resour Bull 7:58–59

McGregor RG (1994) The solid phase controls on the mobility of metals at the Copper Cliff tailings area, near Subdury, Ontario. M.Sc. thesis, University of Waterloo, Waterloo, Ontario

McKnight JF, Fellows ML (1978) Silicate mineral assemblages and their relationship to sulfide mineralization, Piños Altos mineral deposit, New Mexico. Ariz Geol Soc Dig 11:1–8

North RM, McLemore VT (1986) Silver and gold occurrences in New Mexico. N M Bur Mines Miner Resour, Resour Map 15:1–32

Paige S (1910) The ore deposits near Piños Altos, New Mexico. US Geological Survey Bulletin 470; U.S. Government Printing Office, Washington, DC, pp 109–125

Ptacek CJ, Blowes DW (1994) Influence of siderite on the pore-water chemistry of inactive mine tailings impoundments: In Alpers CN, Blowes DW (eds) Environmental geochemistry of sulfide oxidation, ACS Symposium Series 550. American Chemical Society, Washington, DC, pp 172–189

Rollinson HR (1993) Using geochemical data: evaluation, presentation, interpretation. Longman Group Limited, Harlow UK

Shadlum TN, Turpetko SA (1970) Relationship between microhardness and isomorphous iron content in synthetic sphalerite. Dokl Acad Sci USSR Earth Sci 194:141–143

Soulé JH (1948) West Piños Altos Zn-Pb deposits. U.S. Department of Interior, 4237, R.I., U.S. Government Printing Office, Washington, DC, Report of Investigation

Thornton I (ed) (1983) Applied environmental geochemistry. Academic Press, London

Walder IF, Chavez WX (1995) Mineralogical and geochemical behavior of mill tailing material produced from lead-zinc skarn mineralization, Hanover, Grant County, New Mexico, USA. Environmental Geology 26:1–18